



Effect of Temperature on the Iron Sulphur Ratio of Pyrite Deposited by Aerosol Assisted Chemical Vapour Deposition Method

Christian Nweze^{1*}, Masood Akhtar², Mohammad Azad Malik², Paul O'Brien²
and Stella Ezeonu¹

¹Department of Physics and Industrial Physics, Nnamdi Azikiwe University, P.M.B 5025, Awka, Anambra State, Nigeria.

²School of Chemistry and Materials, University of Manchester, England, UK.

Authors' contributions

This work was carried out in collaboration between all authors. Authors MAM and POB designed the study. Author MA prepared the precursor used. Author CN wrote the protocol and first draft processed of the manuscript all the data, interpreted the results, and wrote the manuscript. Authors MM and POB managed the analyses of the work and gave a number of suggestions that significantly improved the paper. Author SE managed the literature searches. All authors read and approved the final manuscript.

Article Information

DOI: 10.9734/PSIJ/2015/12924

Editor(s):

- (1) Daniel Beysens, OPUR International Organization for Dew Utilization, France.
(2) Christian Brosseau, Distinguished Professor, Department of Physics, Université de Bretagne Occidentale, France.

Reviewers:

- (1) Anonymous, Universiti Teknologi Malaysia, Malaysia.
(2) Anonymous, Universidad Autónoma de Nuevo León, Mexico.
(3) Anonymous, Instrument Technology Research Center, Taiwan.
(4) Anonymous, Universiti Sains Malaysia, Malaysia.

Complete Peer review History: <http://www.sciencedomain.org/review-history.php?iid=833&id=33&aid=6925>

Original Research Article

Received 23rd July 2014
Accepted 13th September 2014
Published 14th November 2014

ABSTRACT

Pyrite semiconducting film was deposited on a glass substrate from the single source precursor (Fe (S₂CN(Et)₂)₃) by Aerosol Assisted Chemical Vapour Deposition (AACVD). The p-XRD pattern of the deposited films shows that pure pyrite was deposited at 300 °C whereas mixture of pyrite and marcasite was deposited at 350 °C, 400 °C and 450 °C. EDX analysis shows that semiconducting pyrite was deposited at 300 °C and 350 °C, whereas metallic pyrite was deposited at 400 °C and 450 °C.

*Corresponding author: Email: ci.nweze@unizik.edu.ng;

Keywords: EDX; XRD; SEM; semiconducting pyrite; metallic pyrite; AACVD.

1. INTRODUCTION

Iron pyrite (cubic FeS_2) is a promising photovoltaic (PV) material and has some properties that makes it suitable for photovoltaic application, these solid state properties include, indirect band gap of 0.98eV, optical absorption coefficient of 10^5cm^{-1} (for $\lambda < 900 \text{nm}$), adequate minority carrier diffusion length of (100-1000) nm, essentially infinite elemental abundance, high photocurrent and high quantum efficiencies [1-6]. Pyrite solar cell has some advantages over other photovoltaic materials such as cheap, nontoxic and could make a significant impact even with lower efficiencies, because most of the materials reported as photovoltaic use either toxic or not very abundant elements such as cadmium, lead or indium, etc [7] which means that these materials cannot contribute significantly to a future energy supply. Recent estimates of the annual electricity potential as well as material extraction costs and environmental friendliness led to the identification of materials that could be used in photovoltaic applications on a large scale [8]. The most promising materials include iron and copper sulfides. Various methods have been used to deposit pyrite, such as, flash evaporation [9], metal organic chemical vapour deposition [1], vacuum thermal evaporation [10], ion beam and reactive sputtering [11], chemical vapour deposition [12], electrodeposition [13] and molecular beam deposition [14]. Other methods include chemical spray pyrolysis [15], vapour transport [16], hot injection method [17], sulphurization of iron oxides [18], and plasma assisted sulphurization of iron [19]. Each technique of thin film deposition has its own advantages and disadvantages. Herein, we used solution based method, precisely Aerosol Assisted Chemical Vapour Deposition (AACVD) method to deposit nanocrystals of pyrite from a solution using single source precursor that is Diethyldithiocarbamate iron (III) ($\text{FeS}_2\text{CN}(\text{Et})_2_3$) and characterized the deposited films using XRD and EDX to determine the structure and iron-sulphur ratio of the deposited films. We have previously reported optical properties of pyrite deposited by AACVD from Diethyldithiocarbamate iron (III) and in this research work, we reported the effect of depositing temperature on iron-sulphur ratio.

2. EXPERIMENTAL

All reagents were used as purchased and solvents were distilled prior to use. All syntheses

were performed under an inert atmosphere of dry nitrogen using standard schlenck techniques. Elemental analysis was performed by the University of Manchester micro-analytical laboratory. Mass spectra were recorded on a Kratos concept 1S instrument. Infra-red spectra were recorded on a Specac single reflectance ATR instrument ($4000\text{-}400 \text{cm}^{-1}$, resolution 4cm^{-1}). Melting points were recorded on a Barloworld SMP10 Melting Point Apparatus. p-XRD studies were performed on an Xpertdiffractometer using $\text{Cu-K}\alpha$ radiation. The samples were mounted flat and scanned between 20° and 70° with a step size of 0.05° and various count rates. Films were carbon coated using an Edward's E306A coating system before carrying out EDX analysis. EDX was carried out using a DX4 instrument mounted on Philips XL30 field emission gun scanning electron microscope (FEGSEM)).

2.1 Precursor Synthesis

The precursor, Diethyldithiocarbamate iron (III) was prepared as described previously by Paul O'Brien group and Nair et al. [20,21,22].

2.2 Preparation of Solution

The solution was prepared by dissolving 0.3g (0.6 mmol) of the precursor ($\text{FeS}_2\text{CN}(\text{Et})_2_3$) in 15ml of toluene in a two-necked 100ml round bottom flask and concentration of 0.04mol/dm^3 was achieved. The substrates used were glass microscope slides. The glass slides were cut to size approximately $1 \times 2 \text{cm}^2$ by hand. The substrates were not handled with bare fingers rather with hand gloves to avoid contamination. The substrates were cleaned with detergent solutions, rinsed with distilled water and then rinsed with acetone, methanol and distilled water and finally dried before use.

2.3 Deposition of Thin Films of Pyrite by AACVD

15ml of the solution was poured into the two-necked round bottom flask with a gas inlet that allowed argon (carrier gas) to pass into the solution to aid the transport of the aerosol. A piece of reinforced tubing was used to connect the flask to the reactor tube. Platon flow gauge was used to control argon flow rate. Seven glass substrates (approximately $1 \times 2 \text{cm}^2$) were placed inside the reactor tube which is placed in

a Carbolite furnace maintained at a certain temperature. The precursor solution in a two-necked round bottom flask was kept in a water bath above the piezoelectric modulator of a PIFCO ultrasonic humidifier (Model No 1077). The solution was evaporated and the generated aerosol droplets of the precursor were transferred into the hot wall zone of the reactor by the carrier gas. This precursor vapour reached the heated substrate surface where thermally induced reactions and film deposition took place at 60mins and a particular temperature. The temperature of the Carbolite furnace was varied in step of 50°C starting from 300°C to 450°C. The time was kept at 60mins, the flow rate kept at 160sccm and the concentration kept at 0.04mol/dm³ throughout the experiment. The experiment was repeated a good number of times, (Table 1) summarized the parameter that was varied during the deposition.

3. RESULTS AND DISCUSSION

3.1 XRD Pattern of the Films

The p-XRD patterns of the deposited films are shown in (Fig. 1). From (Fig. 1), the vertical lines represent the standard cubic pyrite pattern (FeS_{1.96} (ICDD No. 01-073-8127)). The film deposited at 300°C (A) corresponds to pure polycrystalline pyrite with no trace of marcasite peak, whereas the films deposited at 350°C (B), 400°C (C) and 450°C (D) show mixture of polycrystalline pyrite and marcasite. The marcasitic peak increases as the deposition temperature increases. The peaks at 26.3°, 39.2°, 52.1° (2θ) correspond to marcasitic peak (ICDD No. 04-003-2016). Major diffraction peaks of the films deposited, both pure and impure

pyrite, lies on (111), (200), (210), (211), (220), (311) and (032) planes of reflection, with the preferred orientation on (200) plane of reflection.

3.2 EDX of the Films

The EDX analysis of all the films shows the presence of Iron and sulfur (Fig. 2). Quantification of iron and sulfur in the films shows that ratio of iron and sulphur increases with temperature. The iron: Sulfur ratio is approximately 50:50 at 300°C and 350°C, 60:40 at 400°C and 64:36 at 450°C (Table 2) this result compares well with the work of Masood et al [23] who reported iron sulfur ratio of 50:50 at 350°C, 50:49 at 400°C and 78:21 at 450°C for (Fe(S₂CNEt^tPr)₃) single source precursor deposited on silicon substrate. This result shows that the deposited semiconducting film changes from semiconducting to metallic film at high temperature. The observed sulphur deficiency at elevated temperature is attributed to the fact that sulphur evaporates from thin films at high temperatures [23,24] and its likely to depend on the nature of the substrate used.

3.3 SEM Images of the Films

The SEM images from the films deposited are shown in (Figs. 3, 4, 5 and 6) for the film deposited at 300°C, 350°C, 400°C and 450°C respectively. At 300°C, the SEM image shows irregular shape crystallites (Fig. 3), at 350°C, clusters of hexagonal plates and irregular shape crystallites is formed (Fig. 4). At 400°C flower like clusters were deposited and it is observed that some crystallites are in the process of transformation (Fig. 5) whereas at 450°C sheet like crystallites were deposited (Fig. 6).

Table 1. Variation of temperature at 60 minutes and 0.04mol/dm³

S/N	Slide no	Argon flow rate (sccm)	Concentration of precursor (mol/dm ³)	Time of deposition (minutes)	Temperature of deposition (°C)	Repeated times
1	A	160.00	0.04	60.00	300.00	3
2	B	160.00	0.04	60.00	350.00	3
3	C	160.00	0.04	60.00	400.00	3
4	D	160.00	0.04	60.00	450.00	3

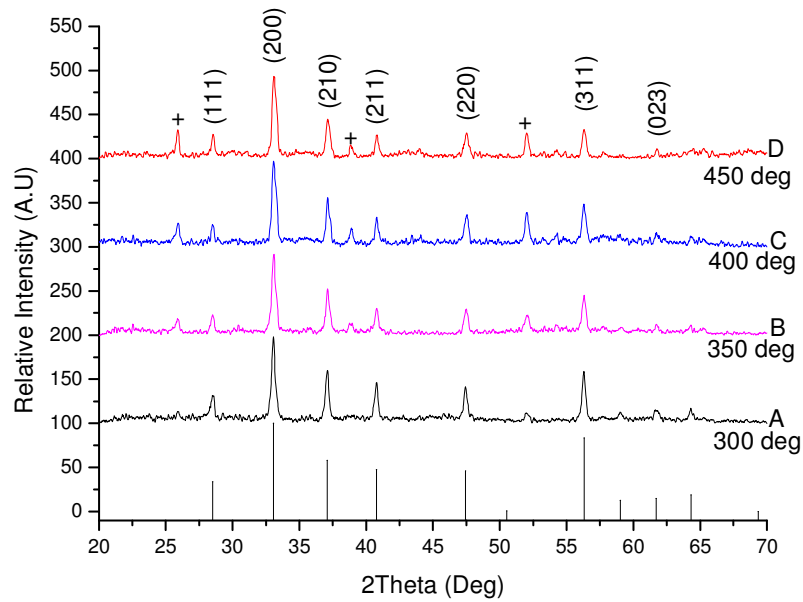


Fig. 1. p-XRD patterns of deposited films, at 300°C (A) pure polycrystalline pyrite ($\text{FeS}_{1.96}$ (ICDD No. 01-073-8127) is formed with planes of reflection on (111), (200), (210), (211), (220), (311) and (023), at 350°C (B), 400°C (C), 450°C (D) mixture of pyrite and marcasite (+) (ICDD No. 04-003-2016) is formed

Table 2. The iron:sulphur ratio for the films deposited at 300°C, 350°C, 400°C and 450°C

Deposition time (minutes)	Temperature							
	300°C		350°C		400°C		450°C	
	Fe %	S %	Fe %	S %	Fe %	S %	Fe %	S %
60	48	52	50	50	60	40	70	30

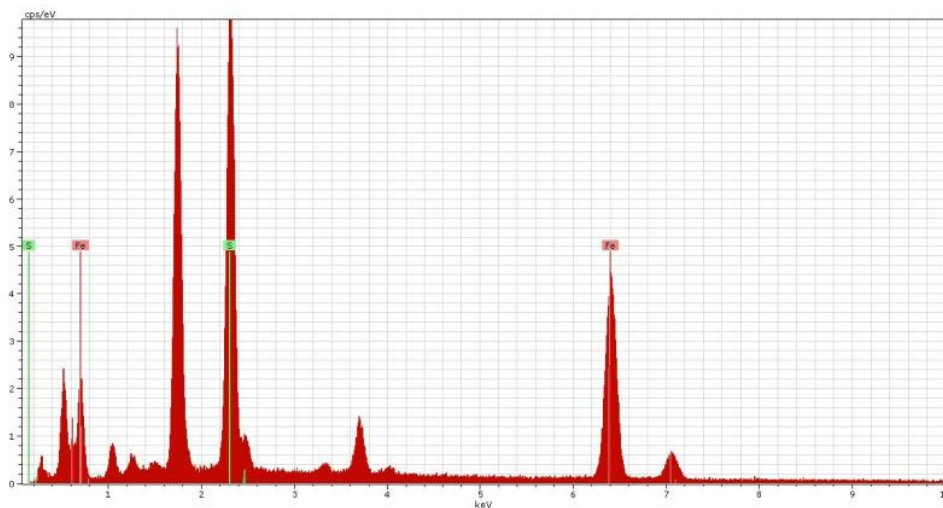


Fig. 2. EDX spectrums of all the films deposited from complex $(\text{Fe}(\text{S}_2\text{CN}(\text{Et})_2)_3)$. The films show the presence of Iron (pink colour) and Sulphur (light green colour)

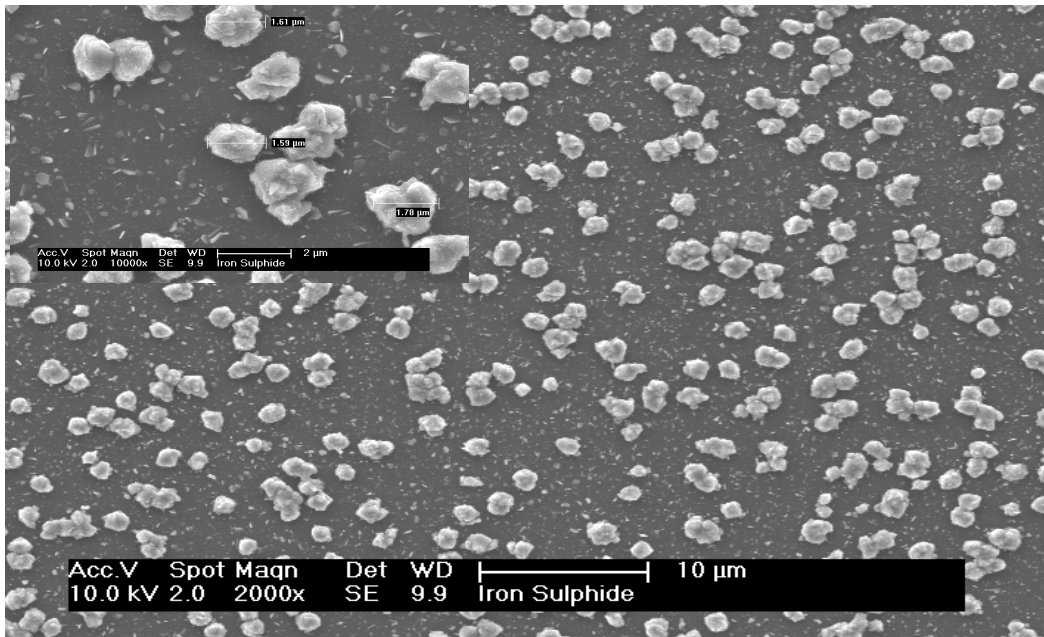


Fig. 3. SEM image of iron sulphide (pyrite $\text{FeS}_{1.96}$) deposited at 300°C

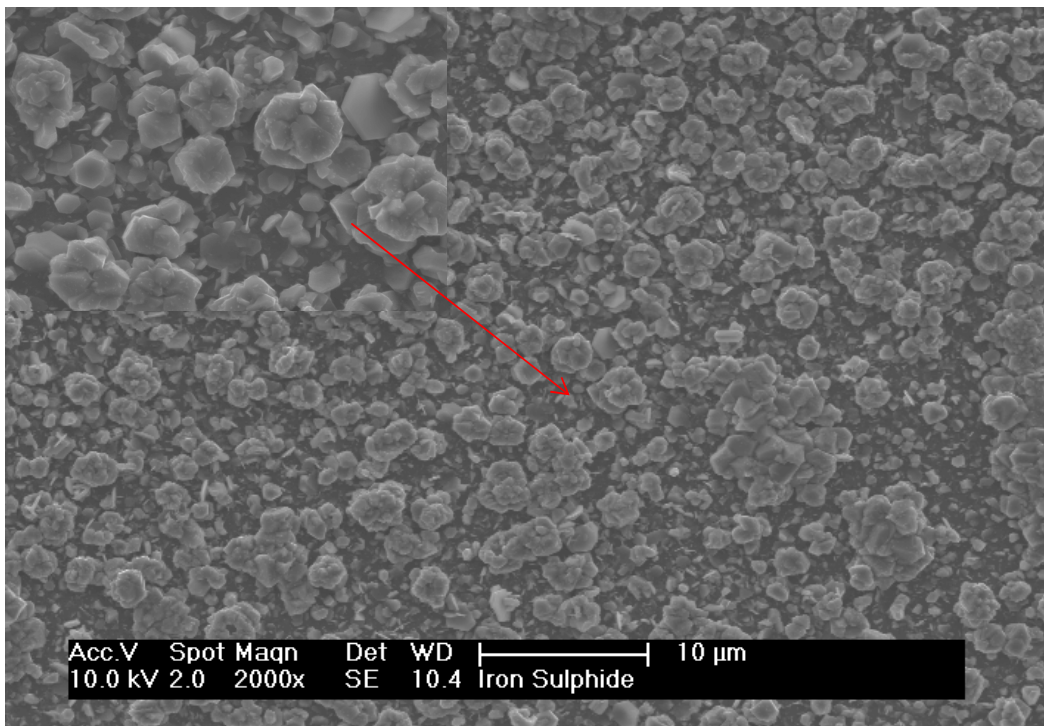


Fig. 4. SEM image of iron sulphide (pyrite $\text{FeS}_{1.96}$) deposited at 350°C

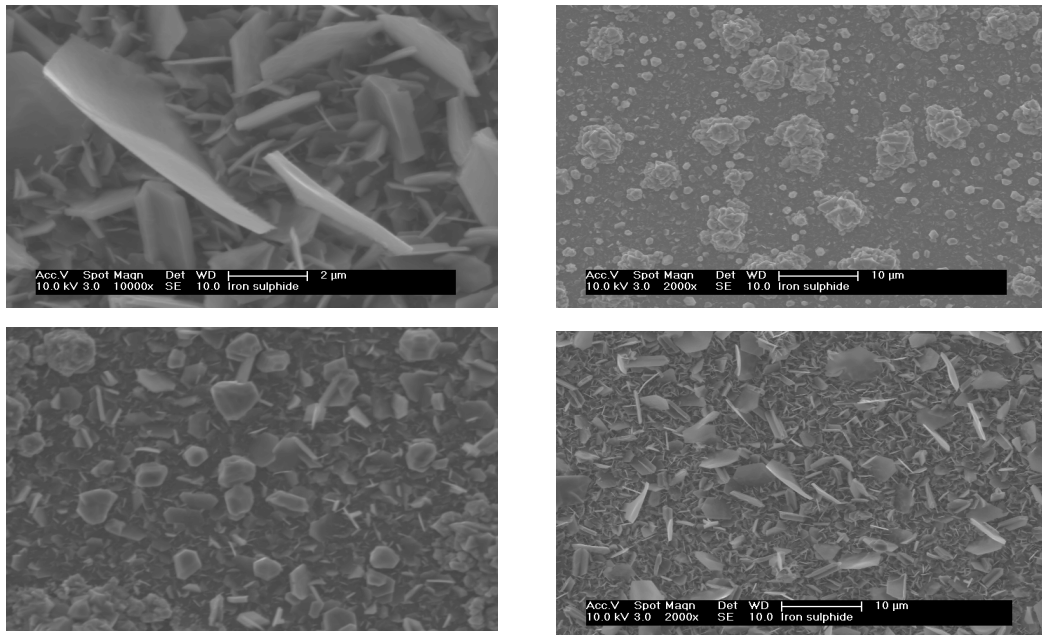


Fig. 5. SEM image of iron sulphide (pyrite $\text{FeS}_{1.96}$) deposited at 400°C

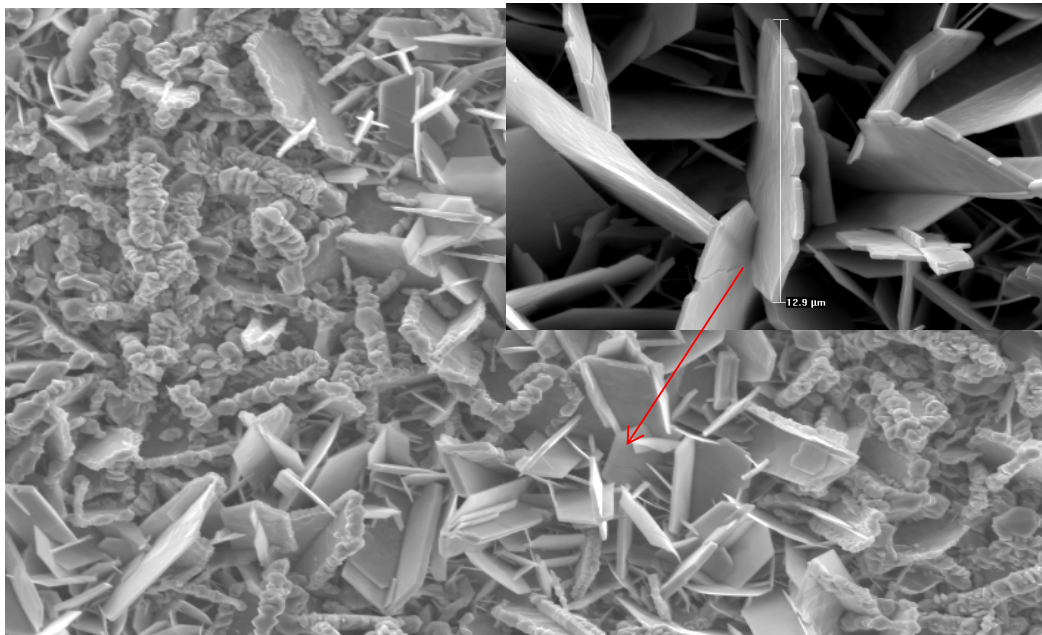


Fig. 6. SEM image of iron sulphide (pyrite $\text{FeS}_{1.96}$) deposited at 450°C

4. CONCLUSION

Semiconducting pyrite was successfully deposited onto glass substrates from the single source precursor $(\text{FeS}_2\text{CN}(\text{Et})_2)_3$ by AACVD method. The p-XRD patterns of the deposited films show that polycrystalline pure pyrite is

formed at 300°C whereas at 350°C, 400°C and 450°C polycrystalline mixture of pyrite and marcasite is formed. We also observed that the deposition temperature has significant effect on the iron:sulfur ratio of the deposited films. The iron:sulfur ratio of 48:52, 50:50, 60:40 and 70:30 were obtained at 300°C, 350°C, 400°C and

450°C respectively. This shows that at high deposition temperature, the pyrite film become metallic. These results show that iron sulfide minerals are typified by a range of significant temperature induced composition and phase transformation.

ACKNOWLEDGEMENTS

The authors are grateful to Tertiary Education Trust Fund (TETFund) for sponsoring this research work. Many thanks to Dr. Chris Wilkinson, Michael Faulkner and Gary Harrison of the University of Manchester for their time in training us on how to use equipment in The School of Material University of Manchester.

COMPETING INTERESTS

Authors have declared that no competing interests exist.

REFERENCES

- Hopfner C, Ellmer K, Ennaoui A, Pettenkofer C, Fiechter S, Tributsch H. Stoichiometry-, phase- and orientation-controlled growth of polycrystalline pyrite (FeS₂) thin films by MOCVD. *Journal of Crystal Growth*. 1995;151.
- Puthussery James, Sean Seefeld, Nicholas Berry, Markelle Gibbs and Matt Law. Colloidal iron pyrite nanocrystal inks for thin-film photovoltaics. *Journal of the American Chemistry Society*. 2011;133, 716.
- Ramasamy K, Malik MA, Helliwell M, Tuna F, O'Brien P. Iron thiobiurets: single-source precursors for iron sulfide thin films. *Inorganic Chemistry*. 2010;49:8495.
- Nicholas Berry, Ming Cheng, Craig L. Perkins, Moritz Limpinsel, Jonh C, Hemminger, Matt Law. Atmospheric-pressure chemical vapour deposition of iron pyrite thin films. *Adv. Energy Mater*. 2012;2:1124.
- Ennaoui A, Tributsch. Energetic characterization of the photoactive pyrite interface. *H. Sol. Energy Mater*. 1986;14,461.
- Smestad G, Ennaoui A, Fiechter S, Tributsch H, Hofmann WK, Birkholz M, Kautek W. Photoactive thin film semiconducting iron pyrite prepared by sulfurization of iron oxides. *Sol. Energy Mater. Sol. Cells*. 1990;20:149.
- Ahmed Lutfi Abdelhady, Mohammad A. Malik, Paul O'Brien, Floriana Tuna, Nickel and Iron Sulfide Nanoparticles from Thiobiurets. *J. Phys. Chem*. 2012;116:2253.
- Wadia A, Alivisatos AP, Kammen DM. Materials availability expands the opportunity for large-scale photovoltaics deployment. *Environ. Sci. Technol*. 2009;43:2072–2077.
- Ferrer IJ, Nevskaja DM, Heras C, Sanchez C. About the band gap nature of Pyrite as determined from optical and photo-electrochemical measurements. *Solid State Commun*. 1990;74:913.
- Rezig B, Dahman H, Kenzari M. Iron pyrite for flexible solar cells. *Renewable Energy*. 1992;2:125.
- Birkholz M, Lichtenberger D, Hopfner C, Fiechter S. Sputtering of thin pyrite films. *Sol. Energy Mater. Sol. Cells*. 1992;27:243.
- Willeke G, Blenk O, Kloc Ch, Bucher E. Preparation and electrical transport properties of pyrite single crystals. *J. Alloys Compd*. 1992;178:181.
- Nakamura S, Yamamoto A. Electrodeposition of pyrite thin films for photovoltaic cells. *Sol. Energy Mater. Sol. Cells*. 2001;65:79.
- Bronold M, Kubala S, Pettenkofer C, Jaegermann W. Thin pyrite films by molecular beam deposition. *Thin Solid Films*. 1997;304:178.
- Smestad G, Da Silva A, Tributsch H, Fiechter S, Kunst M, Meziani N, Birkholz M. Formation of semiconducting Iron Pyrite by Spray Pyrolysis. *Solar Energy Materials*. 1989;18:299.
- Ennaoui A, Schlichtlorel G, Fiechter S, Tributsch H. Vapour phase epitaxial growth of pyrite and evaluation of the carrier collection in liquid-junction solar cell. *Solar Energy Materials and Solar Cells*. 1992;25:169.
- Steinhagen Chet, Taylor B. Harvey, C. Jackson Stolle, Justin Harris, Brian A. Korgel. Pyrite nanocrystal solar cells: promising, or fool's gold? *Journal of Physical Chemistry Letters*. 2012;3:2352.
- Ouertani B, Ouerfelli J, Saadoun M, Bessais B, Ezzaouia H, Bernede JC. Characterization of pyrite thin films synthesized by sulphuration of amorphous iron oxide films pre-deposited into pyrite films. *Material Characterization*. 2005;54:431.

19. Bausch S, Sailer B, Keppner H, Willeke G, Bucher E, Frommeyer G. Preparation of pyrite films by plasma-assisted sulfurization of thin films. *Applied Physics Letters*. 1990;57:25.
20. Akhtar M, Akhtar J, Malik MA, O'Brien P, Tuna F, Raftery J, Helliwell M. Deposition of iron sulphide nanocrystals from single source precursors. *Journal of Materials Chemistry*. 2011;21:9737.
21. Malik MA, Revaprasadu N, O'Brien P. A simple route to the synthesis of core/shell nanoparticles of chalcogenides. *Chemistry of Materials*. 2001;13:913.
22. Nair PS, Radhakrishnan TRN, Kolawole GA. Preparation of CdS nanoparticles using the cadmium(II) complex of N,N'-bis(thiocarbamoyl) hydrazine as a simple single-source precursor. *Journal of Material Chemistry*. 2001;11:1555.
23. Masood Akhtar, Ahmed Lufti Abdelhady, M. Azad Malik, Paul O'Brien. Deposition of iron Sulfide thin films by AACVD from single source precursor. *Journal of Crystal Growth*. 2012;346:106.
24. Chunggaze M, Malik MA, O'Brien P. Deposition of cadmium sulphide thin films from the single-source precursor bis (diethylmonothiocarbamate) cadmium(II) by low pressure metalorganic chemical vapour deposition. *Advanced Materials for Optics and Electronics*. 1997;7:311.

© 2015 Nweze et al.; This is an Open Access article distributed under the terms of the Creative Commons Attribution License (<http://creativecommons.org/licenses/by/4.0>), which permits unrestricted use, distribution, and reproduction in any medium, provided the original work is properly cited.

Peer-review history:

The peer review history for this paper can be accessed here:
<http://www.sciencedomain.org/review-history.php?iid=833&id=33&aid=6925>